

 Open access • Journal Article • DOI:10.2202/1542-6580.2084

Experimental Evaluation of Indirect Heating Tubular Reactors for Solar Methane Pyrolysis — [Source link](#)





Sylvain Rodat, Stéphane Abanades, Gilles Flamant

Published on: 27 Jan 2010 - International Journal of Chemical Reactor Engineering (De Gruyter)

Topics: Methane, Hydrogen production, Natural gas, Kværner-process and Pyrolysis

Related papers:

- [Solar thermal cracking of methane in a particle-flow reactor for the co-production of hydrogen and carbon](#)
- [Solar hydrogen production by thermal decomposition of natural gas using a vortex-flow reactor](#)
- [Solar-thermal dissociation of methane in a fluid-wall aerosol flow reactor](#)
- [A pilot-scale solar reactor for the production of hydrogen and carbon black from methane splitting](#)
- [Co-production of hydrogen and carbon black from solar thermal methane splitting in a tubular reactor prototype](#)

Share this paper:    

View more about this paper here: <https://typeset.io/papers/experimental-evaluation-of-indirect-heating-tubular-reactors-57ogsajlh>

INTERNATIONAL JOURNAL OF CHEMICAL REACTOR ENGINEERING

Volume 8

2010

Article A25

Experimental Evaluation of Indirect Heating Tubular Reactors for Solar Methane Pyrolysis

Sylvain Rodat*

Stéphane Abanades[†]

Gilles Flamant[‡]

*CNRS-PROMES, sylvain.rodats@promes.cnrs.fr

[†]CNRS-PROMES, stephane.abanades@promes.cnrs.fr

[‡]CNRS-PROMES, gilles.flamant@promes.cnrs.fr

Experimental Evaluation of Indirect Heating Tubular Reactors for Solar Methane Pyrolysis*

Sylvain Rodat, Stéphane Abanades, and Gilles Flamant

Abstract

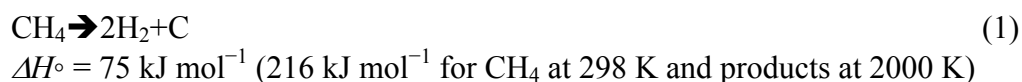
Solar thermal pyrolysis of natural gas is studied for the co-production of hydrogen, a promising energy carrier, and Carbon Black, a high-value nano-material, with the bonus of zero CO₂ emissions. A 10 kW multi-tubular solar reactor (SR10) based on the indirect heating concept was designed, constructed and tested. It is composed of an insulated cubic cavity receiver (20 cm side) that absorbs concentrated solar irradiation through a quartz window by a 9 cm-diameter aperture. The solar concentrating system is the 1 MW solar furnace of CNRS-PROMES laboratory. An argon-methane mixture flows inside four graphite tubular reaction zones each composed of two concentric tubes that are settled vertically inside the cavity. Experimental runs mainly showed the key influence of the residence time and temperature on the reaction extent. Since SR10 design presented a weak recovery of carbon black in the filter, a single tube configuration was tested with an external plasma heating source. Complete methane conversion and hydrogen yield beyond 80% were achieved at 2073K. Hydrogen and carbon mass balances showed that C₂H₂ intermediates affect drastically the carbon black production yield: about half of the initial carbon content in the CH₄ was found as C₂H₂ in the outlet gas. Nevertheless, the carbon black recovery in the filtering device was improved with this new configuration. Data are extrapolated to predict the possible hydrogen and carbon production for a future 50 kW solar reactor. The expected production was estimated to be about 2.47 Nm³/h H₂ and 386 g/h carbon black for 1.47 Nm³/h of CH₄ injected.

KEYWORDS: hydrogen production, concentrated solar energy, methane pyrolysis, solar reactor, plasma reactor, natural gas, carbon black

*This study was funded by the European Project "Solhycarb" (FP6, Contract SES-CT2006-19770). The authors wish to thank J.Y Peroy and J.M. Bienfait for their contribution during the experimental campaign with the plasma reactor, and J.L. Sans, M. Garrabos and O. Prévost for their technical support on SR10.

1. Introduction

Decarbonisation of fossil fuels is the global energy trend to move from solid fossil fuels like coal to liquid and then gaseous fuels, which has to take place during a transition period during which CO₂ emissions intensity should decrease. Hydrogen is the ultimate step and it is viewed as one of the most promising energy carriers to avoid CO₂ emissions (Hefner (2002)). It competes with electricity as a future potential fuel in the transportation sector. Natural gas, which is mainly composed of methane, could make the transition from the today's fossil fuel economy to a future hydrogen economy because it shows the highest H/C ratio among the different hydrocarbons and it already benefits from existing distribution infrastructure (DOE (1999)). Nowadays, production of hydrogen and carbon black are not combined. On the one hand, hydrogen is mainly produced via the steam methane reforming (J.K. Dahl et al. (2004a)), and on the other hand, carbon black is mainly produced from the furnace process (Donnet et al. (1993)). Both processes are responsible for large CO₂ emissions. Various alternatives have been developed in order to dissociate hydrocarbons. High-temperature regenerative gas heaters were investigated by Shpilrain et al. (1999): a matrix is first heated thanks to a combustion chamber, then a carrier gas extracts heat from the pebble bed and finally methane dissociates in the hot carrier gas. Kvaerner Engineering patented a plasma reactor for the production of carbon black and hydrogen from natural gas cracking (Lynum et al. (1993)), and the synthesis of new carbon nanostructures with an innovative plasma technology was also reported (Fulcheri et al. (1997)). The chemistry of the plasma thermal conversion of methane to hydrogen and solid carbon was investigated by Fincke et al. (2002). Atlantic Hydrogen developed a cold arc discharge reactor (Boutot et al. (2007)) to produce hythane (mixture of about 80% methane and 20% hydrogen) claimed as a low emission fuel. Solar thermal methane cracking can also be a solution for the clean co-production of hydrogen and carbon black: about 92% of the pollution associated with the two conventional processes can be eliminated (Wyss et al. (2007)), the remaining emissions stem from the non-renewable electricity used for compressors. It is an interesting solution to replace conventional carbon black processes. The overall reaction can be written as:



Although the dissociation of methane is complete at thermodynamic equilibrium for temperatures beyond 1500K (Hirsch et al. (2001)), other products such as C₂H₂, C₂H₄, and C₂H₆ are generally observed experimentally, which

suggests that a more complex reaction scheme must be considered to explain the production of such species. Consequently, Back et al. (1983) proposed a simplified stepwise dehydrogenation: $2\text{CH}_4 \rightarrow \text{C}_2\text{H}_6 \rightarrow \text{C}_2\text{H}_4 \rightarrow \text{C}_2\text{H}_2 \rightarrow \text{C}$. More detailed kinetic studies also reported refined mechanisms (Fincke et al. (2002), Olsvik et al. (1995), Billaud et al. (1992)).

First solar methane dissociation tests were reported in 1978 (Lédé et al. (1978)), and special interest was given to solar methane cracking for the co-production of hydrogen and carbon black during the last years. Two possible reactor designs were investigated, the direct heating (Kogan et al. (2003), Trommer et al. (2004), Kogan et al. (2004), Hirsch et al (2004), Abanades et al. (2008)) and the indirect heating concepts (Dahl et al. (2004a), Wyss et al. (2007), Dahl et al. (2004b)). The solar irradiated zone is separated from the reacting flow for indirect heating, whereas no separation is used for direct heating, and particle seeding is required for efficient heat transfer to the gas.

This work presents experimental results obtained with a 10 kW solar reactor (SR10) featuring a cubic graphite cavity (behaving as a blackbody cavity) with 4 vertical inside tubular reaction zones. Due to the weak yield of carbon recovery in the filter with this solar reactor prototype, a new design was proposed and tested. Proof-of-concept experiments were performed with a thermal plasma as external heating source (Abanades et al. (2009)) and results showed that this reactor configuration could be applied to a new solar reactor.

2. Solar thermal methane decomposition

2.1. Experimental set-up and solar reactor description

The 10 kW solar reactor was previously described in detail (Rodat et al. (2009a)). The main characteristics of the reactor (Fig. 1) are given in the following section. A graphite cavity receiver serves as a black body solar absorber of cubic shape (20 cm side). Solar radiations enter the reactor through a 9 cm-diameter opening equipped with a domed quartz window. Four independent tubular vertical zones inserted in the graphite cavity are used to carry out the reaction. Each reaction zone, fed independently by a mixture of Ar and CH_4 , is composed of two concentric graphite tubes: an inner tube for gas inlet (12 mm o.d., 4 mm i.d.) and an outer tube for gas outlet (24 mm o.d., 18 mm i.d.). The reactants are fed in the innermost tube whereas the products are evacuated by the annular space between the two tubes; this design enables a preheating of the reactants by the hot products. Conduction losses are lowered thanks to three different insulating layers (first layer of carbon felt, intermediate refractory ceramic fibers, and outer layer of a highly efficient microporous insulator, total thickness: 150 mm). The reactor is designed for a 10kW entering power at nominal conditions. The 1MW solar

furnace of CNRS-PROMES laboratory is used; it can use up to 63 sun-tracking heliostats (45 m² per heliostat) to reflect direct solar radiation toward a parabolic concentrator (1830 m²). At the focal zone, it delivers 9000 suns (1 sun = 1 kW/m²) for full power. The power can be controlled by limiting the number of heliostats and by using a shutter.

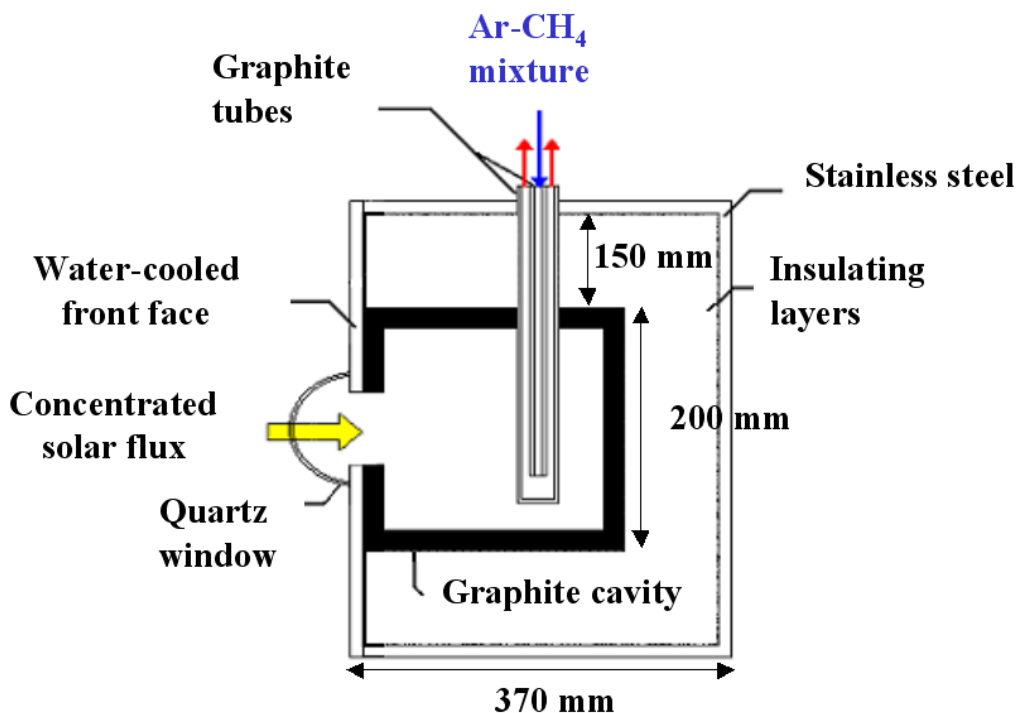


Figure 1. Cross section scheme of the 10 kW solar reactor

During the heating period, the reactor was fed with argon in the tubes until the targeted temperature was reached. Then a controlled mixture of argon and methane was injected in each tube thanks to the use of two mass-flow meters (one for Ar, one for CH₄) for each tube. The temperature was measured by means of a Pt-Rh thermocouple in contact with the graphite cavity wall and by a solar-blind optical pyrometer (wavelength: 5.14 μm) pointing toward the outer wall of a graphite tube inside the cavity through a CaF₂ window. After the tubular reaction zones, the exiting products were mixed together and cooled down thanks to a water-cooled collector. At the exit, the temperature of the gas-particle flow was about 373K and it was directed toward a filter to separate the carbon particles. Each reaction zone was equipped with a pressure sensor at its entrance and the pressure was regulated thanks to a vacuum venturi pump. A part of the filtered

gaseous products was then analyzed with a continuous analyzer for monitoring H₂ and CH₄ concentrations. The methods used for H₂ and CH₄ analysis were thermal conductivity and infrared detections, respectively. A gas chromatograph also measured online the outlet concentration of CH₄, C₂H₆, C₂H₄, C₂H₂, and H₂. The chromatograph (Varian CP 4900) was composed of 2 columns: MolSieve 5A PLOT for H₂ and CH₄, and PoraPLOT U for light hydrocarbons (C₂H_y). The chromatography analysis was based on thermal conductivity detection and the carrier gas was argon, also used as buffer gas during methane cracking experiments, thus eliminating the matrix effects.

2.2. Results with SR10

For each experimental condition, the following parameters are calculated:

- The residence time τ of the gas species is calculated by dividing the volume of the heated part of the tube (part inserted in the graphite cavity for SR10, 240 mm heated length for the tube in the plasma reactor) by the volumetric inlet flow-rate of argon and methane at the real tube temperature and pressure. It is often referred as “space time” (Nauman (2008)). It gives an approximated reaction time because chemical expansion is not included. In the following discussion, “residence time” will always refer to this definition.

$$\tau = \frac{V_r}{Q_0} \quad (2)$$

- The CH₄ conversion gives the proportion of methane that has been transformed and it is defined as:

$$X_{CH_4} = \frac{F_{0,CH_4} - F \cdot y_{CH_4}}{F_{0,CH_4}} \quad (3)$$

- The H₂ yield is the proportion of methane that has been converted into hydrogen and it is calculated from:

$$Y_{H_2} = \frac{F \cdot y_{H_2}}{2 \cdot F_{0,CH_4}} \quad (4)$$

- The C yield is the proportion of methane that has been converted into solid carbon and it is expressed as:

$$Y_C = \frac{F_{0,CH_4} - (F \cdot y_{CH_4} + 2 \cdot F \cdot y_{C_2H_2} + 2 \cdot F \cdot y_{C_2H_4} + 2 \cdot F \cdot y_{C_2H_6})}{F_{0,CH_4}} \quad (5)$$

where F_{0,CH_4} is the inlet molar flow-rate of CH_4 , y_i is the mole fraction of species i , and F is the total outlet flow-rate (including argon as buffer gas) obtained from:

$$F = F_{Ar} + F \cdot y_{CH_4} + F \cdot y_{H_2} + F \cdot y_{C_2H_2} + F \cdot y_{C_2H_4} + F \cdot y_{C_2H_6} \quad (6)$$

F_{Ar} is the molar flow-rate of Ar.

Figure 2 gives the results of cracking experiments concerning natural gas (with 9.5 % ethane and trace amounts of CO_2 and N_2) at 1873K. Four different natural gas inlet flow-rates are reported (8-6-4-2 NL/min), and the argon flow-rate varies so that the natural gas mole fraction in the feed is set to 20%. Consequently, the residence time varies from 11 to 22 ms. When decreasing the methane flow-rate, the off-gas CH_4 mole fraction decreases from 4% to less than 1%. Meanwhile, the H_2 mole fraction increases from 20% to 27%. This increase in reaction efficiency is due to the residence time increase from 11 to 22 ms. The trend for the C_2H_2 off-gas mole fraction is not monotonous. In fact, the C_2H_2 off-gas mole fraction increases when the CH_4 off-gas concentration decreases but remains significant (above 1%). This can be explained by the commonly accepted dehydrogenation mechanism: CH_4 is transformed into C_2H_2 , and the residence time is too short for further reaction. It is confirmed by the last experimental condition with the highest residence time ($\tau=22$ ms), showing the start of C_2H_2 mole fraction decrease. The reaction is kinetically limited. Consequently, the longer the residence time, the higher the conversion. Previous experiments proved that the cracking of natural gas and methane show comparable results (Rodat et al. (2009b)), consequently these experimental results also apply for pure methane.

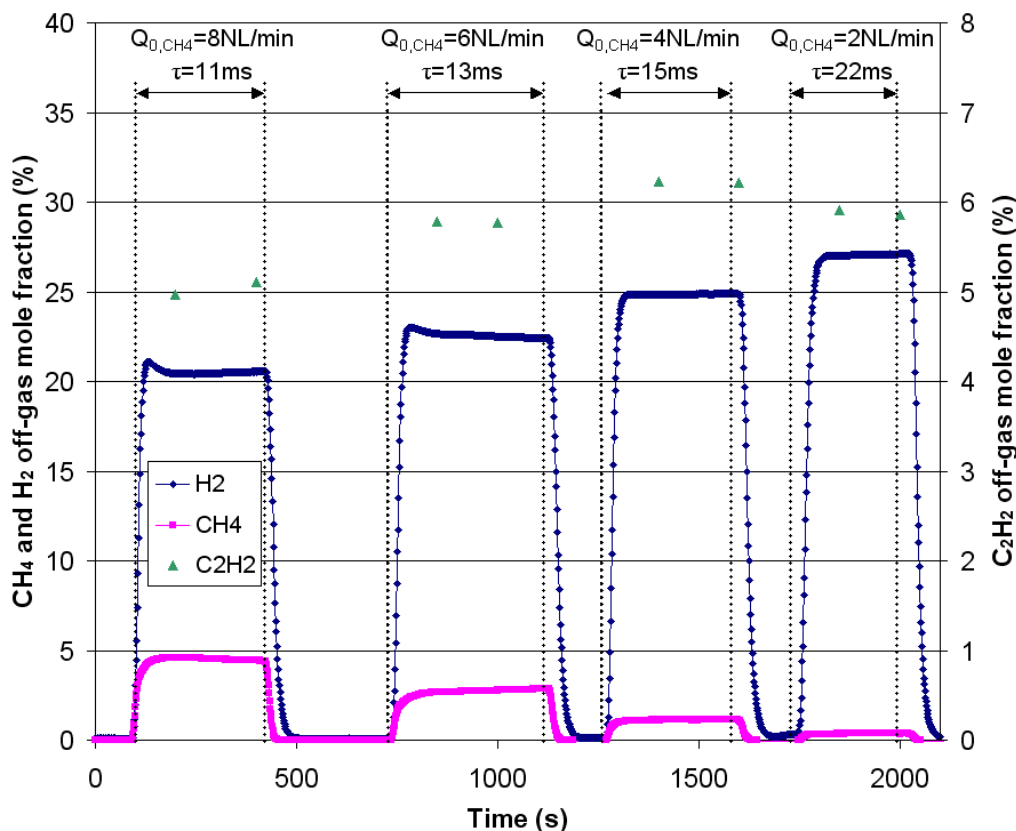


Figure 2. H₂, CH₄ and C₂H₂ off-gas mole fraction for solar natural gas cracking experiments with 20% natural gas in the feed (T=1873K)

Figure 3 shows the results for methane cracking at 2073K. At this temperature, the CH₄ conversion is total for all the experimental conditions tested. Very little discrepancy is observed between the various experimental conditions in terms of H₂ yield (around 80%) but also in terms of C₂H₂ off-gas mole fraction that decreases weakly with residence time: from 5.7% to 4.6 % when τ varies from 9 to 15 ms. These values are very comparable to the ones at 1873K, suggesting that a temperature increase has a weak impact on C₂H₂ dissociation. Nevertheless, a monotonous decrease is observed here, which agrees with the previous comments: the CH₄ conversion is total and consequently increasing the residence time permits only to dissociate the intermediate C₂H₂ species. For a residence time of 22 ms, it was possible to enhance the hydrogen yield (up to 85%) thanks to a better C₂H₂ dissociation (C₂H₂ off-gas concentration of 3.3%). Thus, residence time appears to be the best parameter for enhancing the C₂H₂ dissociation, which is consistent with previously reported results (Choudhary et al. (2003)). The curves presented in both Figures 2 and 3 show that steady state is

rapidly reached (about one minute), and repeated experimental runs (Fig. 3) result in similar off-gas composition, which highlights the results reproducibility and a good control of the experimental parameters, especially the temperature.

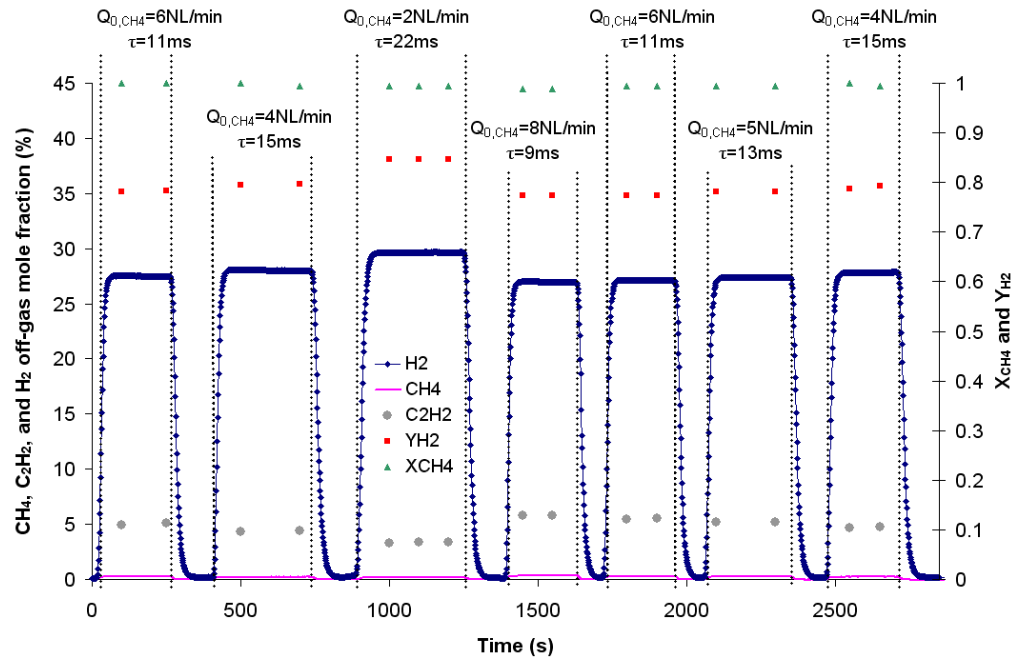


Figure 3. CH₄ conversion, H₂ yield and H₂ and CH₄ off-gas mole fraction for solar methane cracking experiments with 20% methane in the feed (T=2073K)

Results with SR10 were interesting to investigate the production of H₂ but a poor recovery of the carbon in the filter did not allow the detailed study of the carbon black quality (only 2% of the initial carbon content in the feed gas was found as particles in the filter). The carbon deposition due to the upward flow toward the exit is one of the reasons of this problem of evacuation. Consequently, a new tubular design was considered and tested. A preliminary proof-of-concept study was performed by using a thermal plasma as external heating source. The experimental results are commented in the following section.

3. Testing of a new tubular design with an external plasma heating source

3.1. Plasma reactor description

The experimental set-up is displayed in Figure 4. It is very similar to the one described by Fulcheri et al. (1997) but the indirect heating concept is used in the present configuration. The external heating plasma source is located at the top of a cylindrical chamber. It delivers the high-temperature radiative heat needed to dissociate methane in the graphite tube (18 mm i.d., 26 mm o.d., tube length: 600 mm). It is supplied by a 300 kW 3-phase AC generator. Three elementary consumable graphite electrodes (13 mm in diameter) are located at the top of the reactor. Electrode erosion is compensated by a forward movement. The plasma gas (nitrogen, 80 NL/min) is admitted in an annular space between the electrodes and the nozzles, and it produces a large volume of expanded thermal plasma flow inside the chamber. Each of the three electrodes acts successively as an anode and as a cathode. The arc is rotating at the current frequency (1000 Hz). The chamber is a 1.8 m high and 0.28 m i.d. graphite cylinder. The reactor envelope is made of a water-cooled stainless steel vessel. Graphite felt is used to insulate the reactor chamber. Both radiation from the plasma and graphite walls along with the hot nitrogen plasma gas contribute to the tube heating on a 240 mm length. The tube crosses the whole reactor horizontally and it is about 340 mm far from the lowest part of the electrodes. The temperature of the reactor tube depends on operating conditions (mainly electric power and plasma gas flow-rate). The tube wall temperature was 1973K for a current intensity of 80 A (about 45 kW power).

A flow of argon is first fed in the graphite tube to purge oxygen. Then, the plasma is started to heat the tube at the targeted temperature. When the steady state temperature is reached, methane is injected with argon and it dissociates when flowing along the tube. The tube wall temperature is measured thanks to a pyrometer pointing toward the graphite tube. The measurement is carried out through a lateral Pyrex window perpendicular to the reactor tube, the pyrometer is equipped with a filter centred at $\lambda = 0.65 \mu\text{m}$. A flow of N_2 (3 NL/min) is injected tangentially against the window to protect it and to avoid Pyrex overheating. The pyrometer was calibrated, including a correction to account for the transmittance of the Pyrex porthole. After cooling in a water-cooled stainless steel pipe, the products enter a filter to separate carbon particles. The same analysis apparatus as described previously for SR10 are used to analyse the gaseous products. A pressure sensor is positioned at the tube entrance in order to control the pressure in the tube and to detect tube blocking by carbon deposition. The reaction is stopped as soon as a pressure increase is observed.

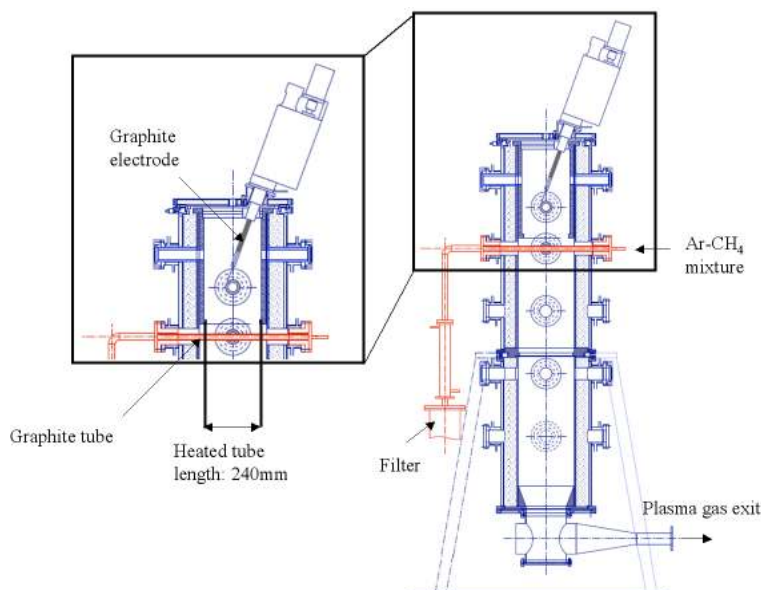


Figure 4. Scheme of the plasma reactor equipped with the reaction tube

3.2. Results and discussion

The influence of the CH_4 mole fraction in the feed, the residence time, and the temperature was investigated in the case of the new tubular configuration to compare with the previous configuration of the multi-tubular solar reactor (Rodat et al. (2009b)). Table 1 reports the results concerning a first set of three experimental conditions at 1893K with a constant residence time of 42 ms (constant total inlet flow rate of 10 NL/min) and an increasing CH_4 mole fraction in the feed. The results show very close CH_4 conversions (70-75%) and H_2 yields (56-61%) whatever the CH_4 mole fraction ranging between 0.1 and 0.3 (the error estimation calculated on X_{CH_4} and Y_{H_2} does not exceed 6%). In the second set of three experimental conditions with a 30% mole fraction of CH_4 in the feed, the total inlet flow rate increases from 4 to 8 NL/min, which leads to a residence time decrease from 50 to 25 ms. The effect of residence time on the CH_4 conversion and the H_2 yield is significant: the decrease of residence time reduces both the CH_4 conversion (from 97 to 80%) and the H_2 yield (from 79 to 69%).

Table 1. Two sets of experimental conditions and corresponding results with the plasma reactor

| Ar (NL/min) | CH ₄ (NL/min) | CH ₄ mole fraction | Tpyrometer (K) | Residence time (s) | H ₂ yield | CH ₄ conversion |
|-------------|--------------------------|-------------------------------|----------------|--------------------|----------------------|----------------------------|
| 9 | 1 | 0.1 | 1893 | 0.042 | 0.56 | 0.70 |
| 8 | 2 | 0.2 | 1893 | 0.042 | 0.61 | 0.75 |
| 7 | 3 | 0.3 | 1893 | 0.042 | 0.61 | 0.74 |
| 2.8 | 1.2 | 0.3 | 1973 | 0.050 | 0.79 | 0.97 |
| 4.2 | 1.8 | 0.3 | 1973 | 0.033 | 0.75 | 0.91 |
| 5.6 | 2.4 | 0.3 | 1973 | 0.025 | 0.69 | 0.80 |

Figure 5 shows the influence of temperature on the CH₄ conversion, H₂ yield and C yield. These reaction performance outputs are all improved when increasing the temperature for a given CH₄ mole fraction. For instance, with a 30% CH₄ in the feed, the CH₄ conversion, H₂ yield and C yield are 99%, 81%, 44% at 2073K and 91%, 73%, 38% at 1973K, respectively. Nevertheless, the temperature variation has no impact on the C₂H₂ content in the off-gas and consequently, the improved C and H₂ yields are directly connected to a decrease in the off-gas CH₄ concentration. These results also confirm that the chemical conversion is not affected by the increase of the CH₄ mole fraction in the feed (up to 50% in Fig. 5), as already observed by Rodat et al. (2009b).

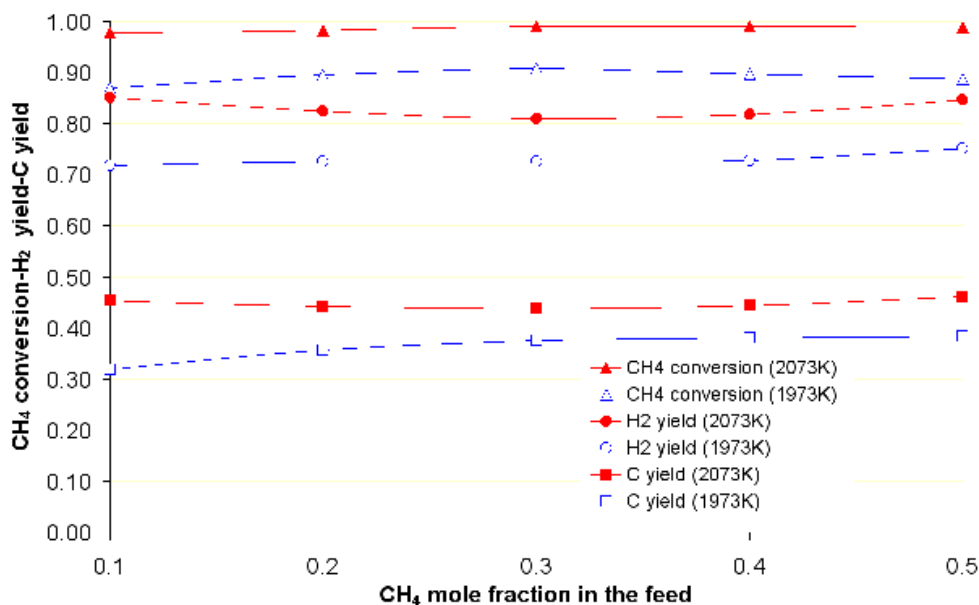


Figure 5. CH₄ conversion, H₂ yield and C yield for similar experiments at 2073K and 1973K

Then, the influence of the tube diameter was investigated. Two different tube diameters, 18 mm i.d. and 15 mm i.d., were tested, the external diameter was identical (26 mm o.d.). To manufacture the tubes, the starting materials were 26 mm-diameter graphite cylinders that were drilled at 15 mm and at 18 mm. Six experimental conditions listed in Table 2 were tested for both tubes (at 1973K). The results presented are related again to the main reactor performance indicators, that is to say, the methane conversion, the hydrogen yield and the carbon yield (Figure 6). The curves show that no significant trend is obtained when comparing the methane conversion and hydrogen yield for each tube in-diameter. The mean discrepancy is less than 3% for X_{CH_4} and Y_{H_2} . Concerning the carbon yield, the mean discrepancy is about 11%, and it seems that the carbon yield is always lower for the smallest in-diameter than for the largest. Actually, the larger the tube in-diameter, the longer the residence time. Previous results showed that C_2H_2 concentration is very sensitive to residence time. As a result, a residence time increase improves both C_2H_2 dissociation and carbon yield. On the one hand, increasing the tube diameter improves the reaction efficiency since the residence time increases (+30%) and it also gives more space for carbon deposition. On the other hand, decreasing the tube diameter leads to higher gas velocities, which may improve particles transportation to the outlet. Anyway, the reactor performance outputs for the two tube configurations remained very close and then, the tube diameter, in the studied range, was not an influencing parameter. This can be explained by the increasing heat transfer coefficient when the diameter decreases. Indeed, the flow in the tube is laminar, and so, for a fully developed temperature profile, the Nusselt number ($\text{Nu} = h \cdot d / \lambda$, with h the heat transfer coefficient ($\text{W}/\text{m}^2 \cdot \text{K}$), d the tube diameter (m) and λ the thermal conductivity ($\text{W}/\text{m} \cdot \text{K}$)) is constant (Rohsenow et al. (1973)). Consequently, since the runs were carried out with similar mixtures, λ is also constant and the ratio between the heat transfer coefficients for the 15 mm i.d. tube ($h_{15\text{mm}}$) and 18 mm i.d. tube ($h_{18\text{mm}}$) corresponds to the diameter ratio. Thus $h_{15\text{mm}}$ is about 20% higher than $h_{18\text{mm}}$, leading to a better heat transfer that can partially compensate a reduced residence time.

Table 2. Experimental conditions (1 to 6) corresponding to Figure 6 (T=1973K)

| | Ar (NL/min) | CH ₄ (NL/min) | CH ₄ mole fraction | Residence time (s) (18mm i.d. / 15mm i.d.) |
|----------|-------------|--------------------------|-------------------------------|---|
| 1 | 4.5 | 1 | 0.18 | 0.036 / 0.022 |
| 2 | 4.5 | 1.5 | 0.25 | 0.033 / 0.020 |
| 3 | 4.5 | 2 | 0.31 | 0.031 / 0.019 |
| 4 | 5.6 | 1.4 | 0.20 | 0.029 / 0.020 |
| 5 | 4.9 | 2.1 | 0.30 | 0.029 / 0.020 |
| 6 | 4.2 | 2.8 | 0.40 | 0.029 / 0.020 |

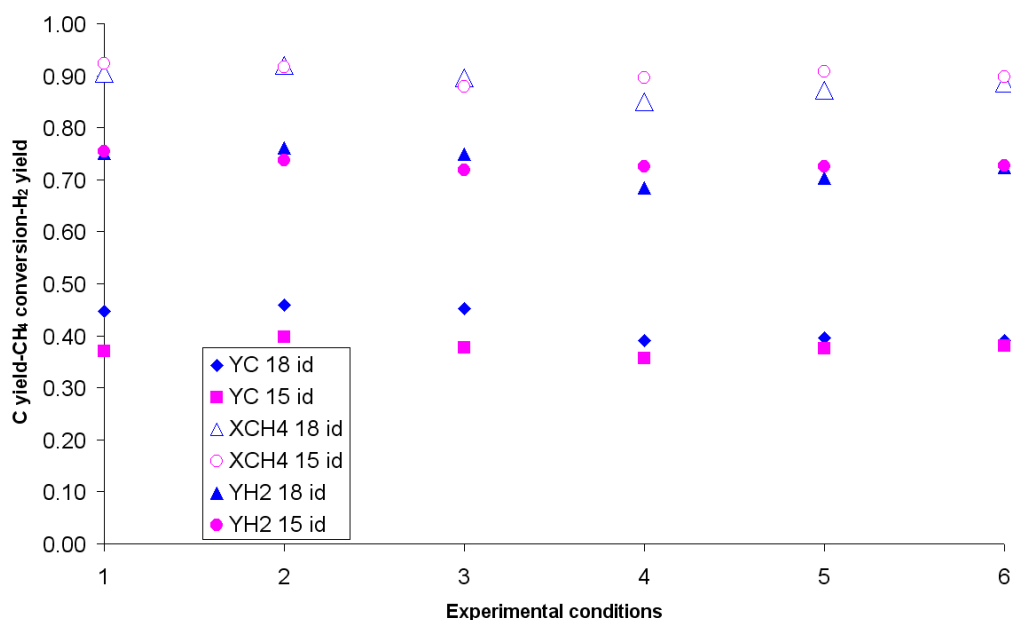


Figure 6. Comparison of the carbon yield (Y_C), methane conversion (X_{CH_4}) and hydrogen yield (Y_{H_2}) for 6 different experimental conditions either with a tube of 15 mm i.d. or 18 mm i.d.

Figure 7 plots the H₂, CH₄, and C₂H₂ mole fraction for an experimental run at 2073K and a methane mole fraction in the feed varying between 10 and 50%. The total flow-rate is kept constant at 7 NL/min, in order to guarantee similar residence times for each condition. When increasing the methane mole fraction in the feed, the H₂ off-gas mole fraction increases significantly. The same trend is observed for CH₄ and C₂H₂ but the variations are smaller. Finally, the

CH₄ conversion exceeds 98% in every cases, whereas the H₂ yield oscillates between 81% and 85%. Thus, a high conversion can be maintained for methane mole fractions up to 50%, which leads to better reactor thermal efficiencies. Nevertheless, previous results showed that a dilution of methane is mandatory in order to delay carbon deposit. At the end of the experiment (start of clogging after 2500 s), the H₂ production increases rapidly whereas the C₂H₂ and CH₄ off-gas mole fractions diminish. This increase in methane dissociation is typical of a residence time increase. It is explained by a pressure increase in the tube due to carbon deposit and tube blocking. The experiment was thus stopped and the tube was cleaned. Solutions can be proposed, especially concerning the problem of carbon deposit, for process implementation in large scale solar plants and continuous operation. Common CB processes operate with very high velocities (between 0.3 and 0.8 Mach) (Donnet et al. (1993)) thus the carbon deposition issue is highly diminished. At laboratory scale, it is not possible to work with such velocities without decreasing drastically the residence time, thus the CH₄ dissociation efficiency. Current investigations at larger scale suggest that a turbulent flow should be preferred in order to increase both heat and mass transfers and carbon particle transport. In order to maintain suitable residence time (at least 50 to 100 ms), long tubes are envisaged. In addition, the carbon black industry has also to face the carbon deposition issue, which is solved by combustion with oxygen. In our case, the material used for the tubes is graphite, which is not suitable in the presence of oxygen. Thus, two possible solutions could be proposed, consisting in using either a material that withstand oxidation (alumina is used industrially) or a mechanical cleaning.

A mass balance on hydrogen and carbon was achieved based on the results presented in Figure 7. The mass balances were obtained by integrating these data.

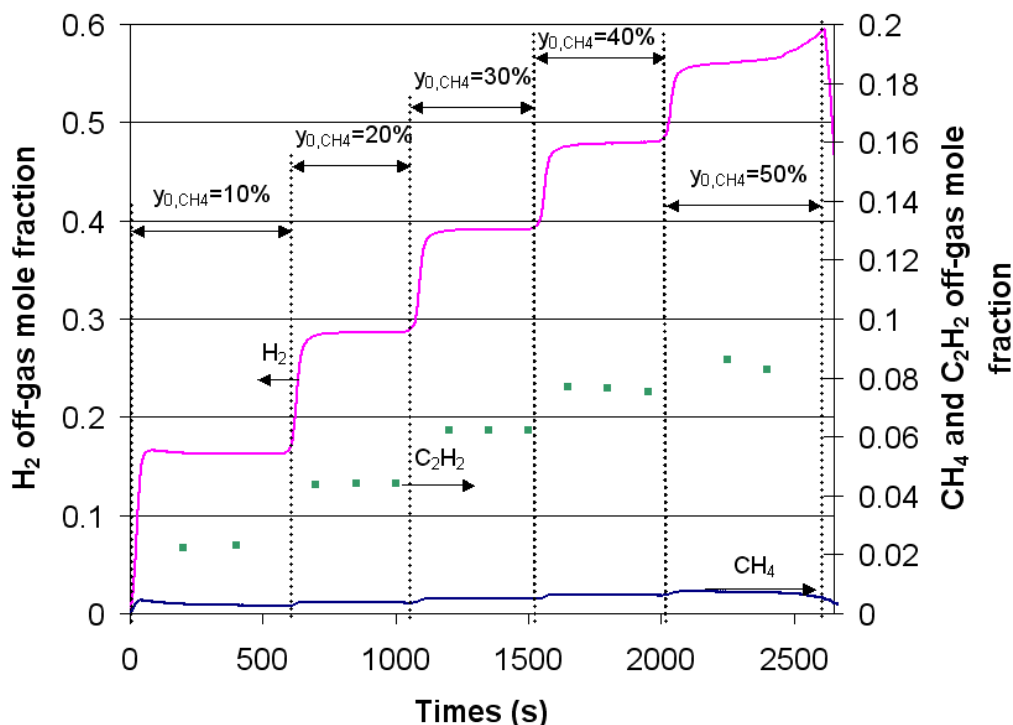


Figure 7. H₂, CH₄ and C₂H₂ off-gas mole fraction for methane cracking experiments (plasma reactor) with a total fed flow-rate of 7 NL/min (T=2073K)

The reactor tubes and the filter were weighted before and after experiments. The mass of carbon accumulated in the tubes was 14.4 g, while 9.91 g of carbon was recovered in the filter. A total of 92.7 NL of methane was introduced in the reactor. Then, a mass balance between the recovered solid carbon and the amounts of C and H contained in the exhaust gaseous species shows that nearly 100% of the initial carbon mass and 97% of the initial hydrogen mass are retrieved at the exit according to the following calculations (only H₂, C, CH₄, and C₂H₂ are taken into account because the other hydrocarbons show negligible amounts):

$$C(\text{ratio}) = \frac{\frac{m_{CH_4}}{M_{CH_4}} + \frac{2m_{C_2H_2}}{M_{C_2H_2}} + \frac{m_C}{M_C}}{\frac{m_{0,CH_4}}{M_{0,CH_4}}} \quad (12)$$

$$H(\text{ratio}) = \frac{\frac{4m_{CH_4}}{M_{CH_4}} + \frac{2m_{C_2H_2}}{M_{C_2H_2}} + \frac{2m_{H_2}}{M_{H_2}}}{\frac{4m_{0,CH_4}}{M_{0,CH_4}}} \quad (13)$$

According to the H mass balance (Fig. 8), 84% of H atoms is found as H₂ gas, 12% is in the form of C₂H₂, 1% is contained in the unconverted CH₄, and the remaining 3% is thus attributed to other hydrocarbons. Consequently, CH₄ is efficiently converted into H₂ (84% of H₂ yield).

Concerning the C mass balance (Fig. 9), 50 % of the carbon is contained in C₂H₂. 49% of the carbon is recovered as solid carbon either in the reactor tubes (29%) or in the filter (20%). Thus, it is possible to recover 10 times the quantity of carbon that was recovered with SR10. 1% of carbon stays in the unconverted CH₄. Methane is not as well converted into solid carbon as it is in H₂ due to the substantial presence of C₂H₂. This suggests that C₂H₂ should be recycled in the process if C is the targeted material.

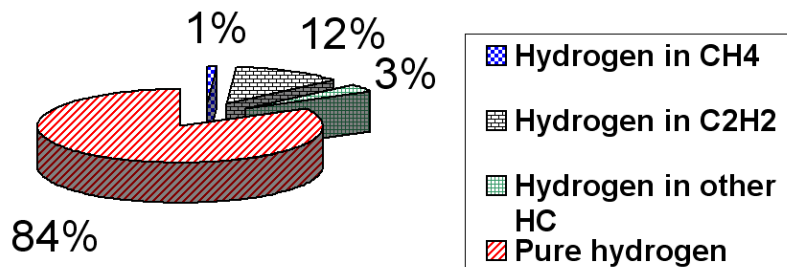


Figure 8. H mass balance (T=2073K, total fed flow-rate: 7 NL/min)

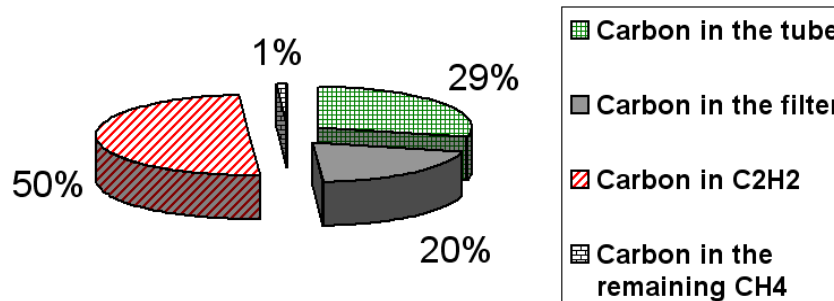


Figure 9. C mass balance (T=2073K, total fed flow-rate: 7 NL/min)

This tubular design will be selected in a 50 kW solar reactor composed of 7 tubes. According to the mean mass balances discussed above (84% H₂ yield and 49% C yield), one can expect the production of 41.2 NL/min of H₂ and 6.4 g/min of carbon black if each tube is fed with 3.5 NL/min of CH₄. Thus, it would be possible to produce sufficient amounts of carbon black (several dozens of grams) that are required for determining precisely its properties (especially mechanical and electrical properties). Moreover, these samples should be more representative of the materials that could be produced with such a solar process.

4. Conclusion

Two different configurations of indirect heating tubular reactor for natural gas pyrolysis were tested experimentally. The first reported experimental results are related to a 10 kW solar reactor for natural gas (or methane) pyrolysis. The four tubular reaction zones were each composed of two concentric tubes positioned vertically. This configuration showed good performances concerning hydrogen production efficiency, but it did not permit to recover efficiently the carbon black in the filter. The positive effect of increasing either the temperature and/or the residence time on the methane pyrolysis was demonstrated. Then, in order to facilitate the gas-solid flow and alleviate the particle deposition issue, a new tubular configuration consisting of a single horizontal tube was proposed and tested by using an external plasma heating source. Significant quantities of carbon particles were collected in the filter bag while a high methane conversion was maintained. The influence of the methane mole fraction in the feed was analysed. Increasing the methane mole fraction in the feed did not alleviate the methane conversion, although a dilution was still required to delay the carbon deposit. This design was selected for the development of a 50 kW pilot solar reactor. The expected production was estimated to be about 2.47 Nm³/h H₂ and 386 g/h carbon black for 1.47 Nm³/h of CH₄ injected. Thus, the expected amount of carbon produced will be sufficient for a thorough analysis of the carbon black properties with respect to the commercial standards.

Nomenclature

| | |
|------------------|--|
| F | total molar flow-rate (mol/s) |
| F _i | molar flow-rate of species i (mol/s) |
| F _{0,i} | inlet molar flow-rate of species i (mol/s) |
| ΔH° | standard reaction enthalpy (J/mol) |
| m _{0,i} | inlet mass of species i (g) |

| | |
|------------|---|
| m_i | mass of species i (g) |
| M_i | molecular weight of species i (g/mol) |
| NL | Normal Liter (at normal conditions: 101.325 kPa and 273.15 K) |
| Q_0 | volumetric inlet flow-rate of argon and methane at the actual tube temperature and pressure (T,P) (m^3/s) |
| V_r | volume of the isothermal part of the tubes where the reaction occurs (m^3) |
| X_{CH_4} | methane conversion |
| Y_C | carbon yield |
| Y_{H_2} | hydrogen yield |
| y_i | mole fraction of species i |

Greek letters

τ space time (s)

References

- Abanades S., Flamant G., "Hydrogen production from solar thermal dissociation of methane in a high-temperature fluid-wall chemical reactor", *Chemical Engineering and Processing: Process Intensification*, 2008, 47, 3, 490-498.
- Abanades S., Tescari S., Rodat S., Flamant G., "Natural gas pyrolysis in double-walled reactor tubes using plasma arc or concentrated solar radiation as external heating source", *Journal of natural gas chemistry*, 2009, 18, 1, 1-8.
- Back M.H., Back R.A., "Thermal decomposition and reactions of methane". In: Albright LF, Crynes BL, Corcoran WH., editors. *Pyrolysis: theory and industrial practice*. New York: Academic Press; 1983, 1-24.
- Billaud F., Guéret G., Weill J., "Thermal decomposition of pure methane at 1263 K. Experiments and mechanistic modelling", *Thermochim Acta*, 1992, 211, 303-322.
- Boutot T.J., Buckle K., Collins F.X., Claus S.J., Estey C.A., Fraser D.M., Liu Z., Whidden T.K., "Decomposition of Natural Gas or Methane Using Cold Arc Discharge", *Atlantic Hydrogen*, WO2007/019664 A1, 2007.
- Choudhary T.V., Aksoylu E., Goodman D.W., "Nonoxidative activation of methane", *Catalysis Reviews*, 2003, 45, 1, 151-203.

Dahl J.K., Buechler K.J., Finley R., Stanislaus T., Weimer A.W., Lewandowski A., Bingham C., Smeets A., Schneider A., "Rapid solar-thermal dissociation of natural gas in an aerosol flow reactor", *Energy*, 2004a, 29, 5-6, 715-725.

Dahl J.K., Buechler K.J., Weimer A.W., Lewandowski A., Bingham C., "Solar-thermal dissociation of methane in a fluid-wall aerosol flow reactor", *International Journal of Hydrogen Energy*, 2004b, 29, 7, 725-736.

DOE (Department of Energy). "A multi-year plan for the hydrogen R&D program. Rationale, structure and technology roadmaps. Office of Power Delivery and Office of Power Technologies", US Department of Energy, 1999.

Donnet J.B., Bansal R.C., Wang M.J., "Carbon Black", Second edition, Revised and expanded, Science and Technology, 1993.

Fincke J.R., Anderson R.P., Hyde T.A., Detering B.A., "Plasma pyrolysis of methane to hydrogen and carbon black", *Industrial and Engineering Chemistry Research*, 2002, 41, 6, 1425-1435.

Fulcheri L., Schwob Y., Flamant G., "Comparison of new carbon nanostructures produced by thermal plasma with industrial Carbon black grades", *Journal de Physique III, France*, 1997, 7, 491-503.

Hefner A.R., "The age of energy gases", *International Journal of Hydrogen Energy*, 2002, 27, 1, 1-9.

Hirsch D., Epstein M., Steinfeld A., "The solar thermal decarbonization of natural gas", *International Journal of Hydrogen Energy*, 2001, 26, 10, 1023-1033.

Hirsch D., Steinfeld A., "Solar hydrogen production by thermal decomposition of natural gas using a vortex-flow reactor", *International Journal of Hydrogen Energy*, 2004, 29, 1, 47-55.

Kogan A., Kogan M., Barak S., "Production of hydrogen and carbon by solar thermal methane splitting. II. Room temperature simulation tests of seeded solar reactor", *International Journal of Hydrogen Energy*, 2004, 29, 12, 1227-1236.

Kogan M., Kogan A., "Production of hydrogen and carbon by solar thermal methane splitting. I. The unseeded reactor", *International Journal of Hydrogen Energy*, 2003, 28, 11, 1187-1198.

Lédé J., Weber C., Villermaux J., “Evaluation of the efficiency of a device which uses solar energy to apply thermal shocks to gas”, Academie des Sciences (Paris), Comptes Rendus, Serie B - Sciences Physiques, 1978, 286, 22, 299-302.

Lynum S., Hox K., Haugsten K., Langoy J., “System for the production of carbon black”, Kvaerner Engineering, 1993, WO 93/20153.

Nauman E.B., “Residence time theory”, Ind. Eng. Chem. Res., 2008, 47, 3752-3766.

Olsvik O., Rokstad O.A., Holmen A., “Pyrolysis of methane in the presence of hydrogen”, Chem. Eng. Technol., 1995, 18, 349- 358.

Rodat S., Abanades S., Coulié J., Flamant G., “Kinetic modelling of methane decomposition in a tubular solar reactor”, Chemical Engineering Journal, 2009a, 146, 1, 120-127.

Rodat S., Abanades S., Flamant G., “High-Temperature Solar Methane Dissociation in a Multitubular Cavity-Type Reactor in the Temperature Range 1823-2073 K”, Energy & Fuels, 2009b, 23, 2666-2674.

Rohsenow W.M., J.P. Hartnett, “Handbook of heat transfer”, 1973.

Shpilrain E.e., Shterenberg V.Y., Zaichenko V.M., “Comparative analysis of different natural gas pyrolysis methods”, International Journal of Hydrogen Energy, 1999, 24, 7, 613-624.

Trommer D., Hirsch D., Steinfeld A., “Kinetic investigation of the thermal decomposition of CH₄ by direct irradiation of a vortex-flow laden with carbon particles”, International Journal of Hydrogen Energy, 2004, 29, 6, 627-633.

Wyss J., Martinek J., Kerins M., Dahl J.K., Weimer A., Lewandowski A., Bingham C., “Rapid Solar-thermal Decarbonization of Methane in a Fluid-wall Aerosol Flow Reactor – Fundamentals and Application”, International journal of chemical reactor engineering, 2007, 5, Article A69.